ADVANCED MATERIALS
www.advmat.de

Responsive Assembly of Upconversion Nanoparticles for pH-Activated and Near-Infrared-Triggered Photodynamic Therapy of Deep Tumors

*Fangyuan Li, Yang Du, Jianan Liu, Heng Sun, Jin Wang, Ruiqing Li, Dokyoon Kim, Taeghwan Hyeon, and Daishun Ling**

Upconversion nanoparticle (UCNP)-mediated photodynamic therapy has shown great effectiveness in increasing the tissue-penetration depth of light to combat deep-seated tumors. However, the inevitable phototoxicity to normal tissues resulting from the lack of tumor selectivity remains as a major challenge. Here, the development of tumor-pH-sensitive photodynamic nanoagents (PPNs) comprised of self-assembled photosensitizers grafted pH-responsive polymeric ligands and UCNPs is reported. Under neutral pH conditions, photosensitizers aggregated in the PPNs are self-quenched; however, upon entry into a tumor microenvironment with lower pH, the PPNs not only exhibit enhanced tumor-cell internalization due to charge reversal but also are further disassembled into well-dispersed nanoparticles in the endo/lysosomes of tumor cells, enabling the efficient activation of photosensitizers. The results demonstrate the attractive properties of both UCNP-mediated deep-tissue penetration of light and high therapeutic selectivity in vitro and in vivo.

Photodynamic therapy (PDT) has been widely applied to oncotherapy because of its minimally invasive nature and spatiotemporally controlled treatment capability.[1] However, the limited tissue-penetration depth of visible light prevents the broad clinical application of PDT.[2] Recently, lanthanide ion-doped upconversion nanoparticles (UCNPs),[3] which absorb near-infrared (NIR) light and subsequently emit the high-energy visible light,[4] have been utilized as nanotransducers for deep-tissue PDT in vivo.[5] However, such PDT agents still have side effects due to deficiencies in selective accumulation at tumor sites and unavoidable activation of photosensitizers under white-light exposure or by self-catalyzed reactions.[6] As a result, patients are required to avoid exposure to daylight, which increases the burden of patients undergoing the PDT treatment.[7] Recently, various photosensitizers (PSs)[8] capable of selective activation by tumor-associated stimuli,[9] such as pH,[10] H_2O_2,[11] glutathione,[12] and enzymes,[13] have been developed. Although triggering sources of visible light are still involved, engineered systems relying on additional internal stimuli would confer greatly enhanced safety for PDT. However, thus far, there are few studies focused on internal-stimuli-responsive PDT agents based on UCNPs, which would be very beneficial for selective PDT of deep tumors, given that they would only be activated at tumor sites and subsequently triggered by NIR light.

Here, we developed tumor-pH-sensitive photodynamic nanoagents (PPNs) comprised of self-assembled photosensitizers grafted pH-responsive polymeric ligands (PPLs) and UCNPs. The PPNs are negatively charged without any discernible photoactivity at normal blood pH of ≈7.4, but can quickly switch their surface charge from negative to positive at an extracellular tumor pH of ≈6.5, and are further disassembled into individual UCNPs at intracellular tumor endo/lysosome pH (≈5.5). This disassembly process promotes the dissociation of the aggregated PSs (self-quenched state) into extended free molecules (dequenched state), enabling significantly enhanced photoactivity of the PSs (**Figure 1**a). Upon NIR irradiation, upconverted emission light from the UCNPs can induce the photoactivity of the free PSs in acidic tumor microenvironment (Figure 1b). Moreover, the strong upconversion luminescence (UCL) from the PPNs can be utilized for imaging-guided PDT. Based on their unique properties involving pH-activated structural switching, we successfully demonstrate the selective PDT of deep-seated tumors.

Dr. F. Li, Y. Du, H. Sun, J. Wang, R. Li, Prof. D. Ling
Institute of Pharmaceutics
College of Pharmaceutical Sciences
Zhejiang University
Hangzhou, Zhejiang 310058, P. R. China
E-mail: lingds@zju.edu.cn
Dr. J. Liu, Dr. D. Kim, Prof. T. Hyeon
Center for Nanoparticle Research
Institute for Basic Science (IBS)
Seoul 08826, Republic of Korea
Prof. T. Hyeon
School of Chemical and Biological Engineering
Seoul National University
Seoul 08826, Republic of Korea
Prof. D. Ling
Key Laboratory of Biomedical Engineering of the Ministry of Education
College of Biomedical Engineering & Instrument Science
Zhejiang University
Hangzhou, Zhejiang 310027, P. R. China
The ORCID identification number(s) for the author(s) of this article can be found under https://doi.org/10.1002/adma.201802808.

DOI: 10.1002/adma.201802808

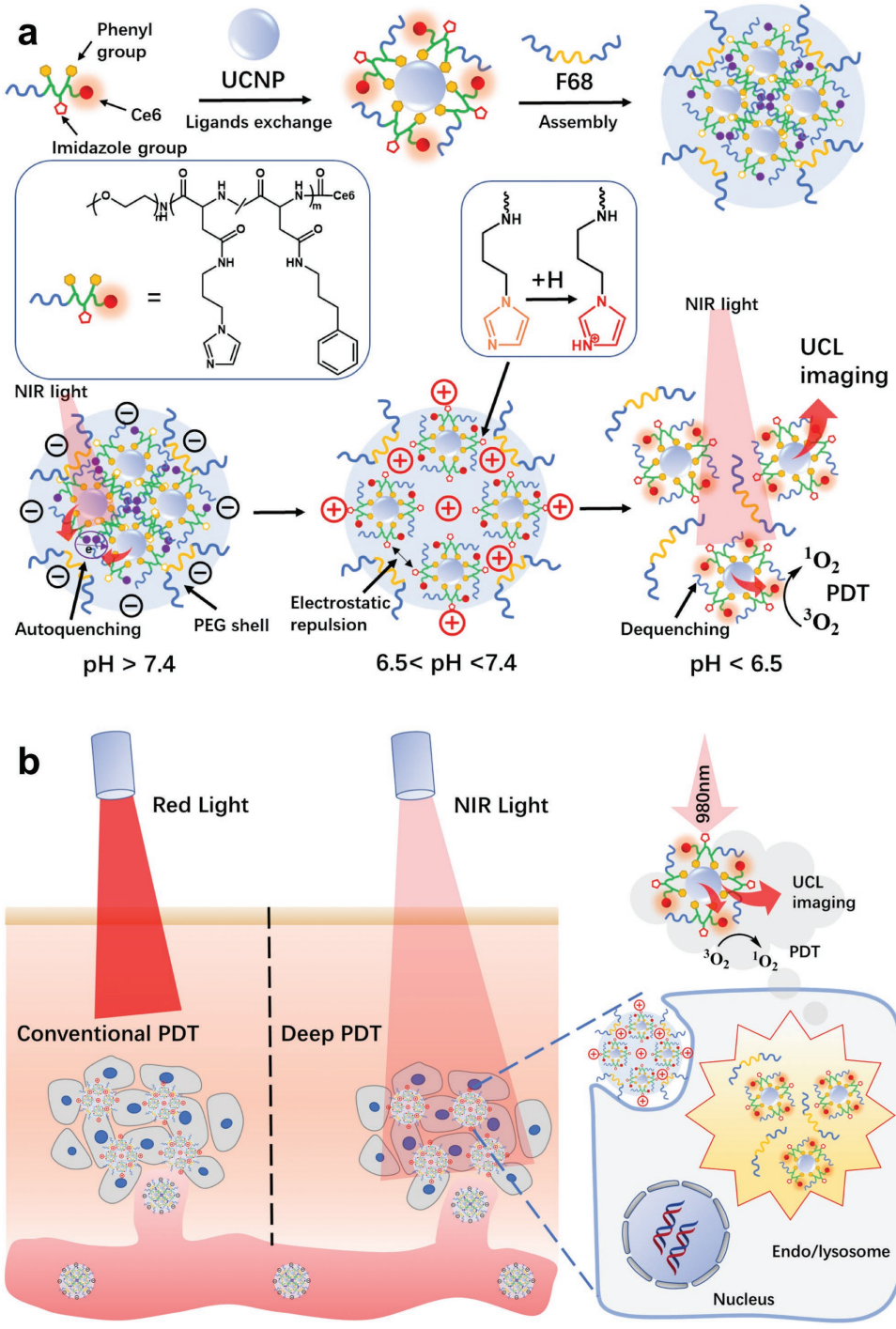

Figure 1. Design and mechanism associated with tumor-pH activation of PPNs. a) Schematic illustration of pH responsive ligand-assisted assembly of UCNPs. b) Schematic representation of tumor-pH-responsive deep tissue PDT.

To fabricate the PPNs, α-$NaYF_4$:Yb(80%),Er(2%)@CaF_2 core@shell nanoparticles were selected as nanotransducers for PDT, because the red-emission intensity from these UCNPs is 15 times higher than well-known β-phase core/shell UCNPs and is suitable for the activation of PS chlorin e6 (Ce6).[14] To impart PPNs with responsiveness to tumor acidic microenvironment, PPLs were prepared by derivatizing poly(ethylene glycol)–poly(β-benzyl-L-aspartate) with 1-(3-aminopropyl) imidazole (API), 3-phenyl-1-propylamine (PPA), and Ce6. The assembly of UCNP/PPLs was achieved using a ligand-assisted strategy. First, UCNPs dispersed in chloroform were added dropwise to the acid–water solution containing PPLs. Upon ultrasonication, the formation of a nanoemulsion occurred, resulting in effective encapsulation of the UCNPs. The mixture was then stirred at room temperature for 1 h before the complete evaporation of chloroform at 60 °C. Second, Pluronic F68 (F68), an

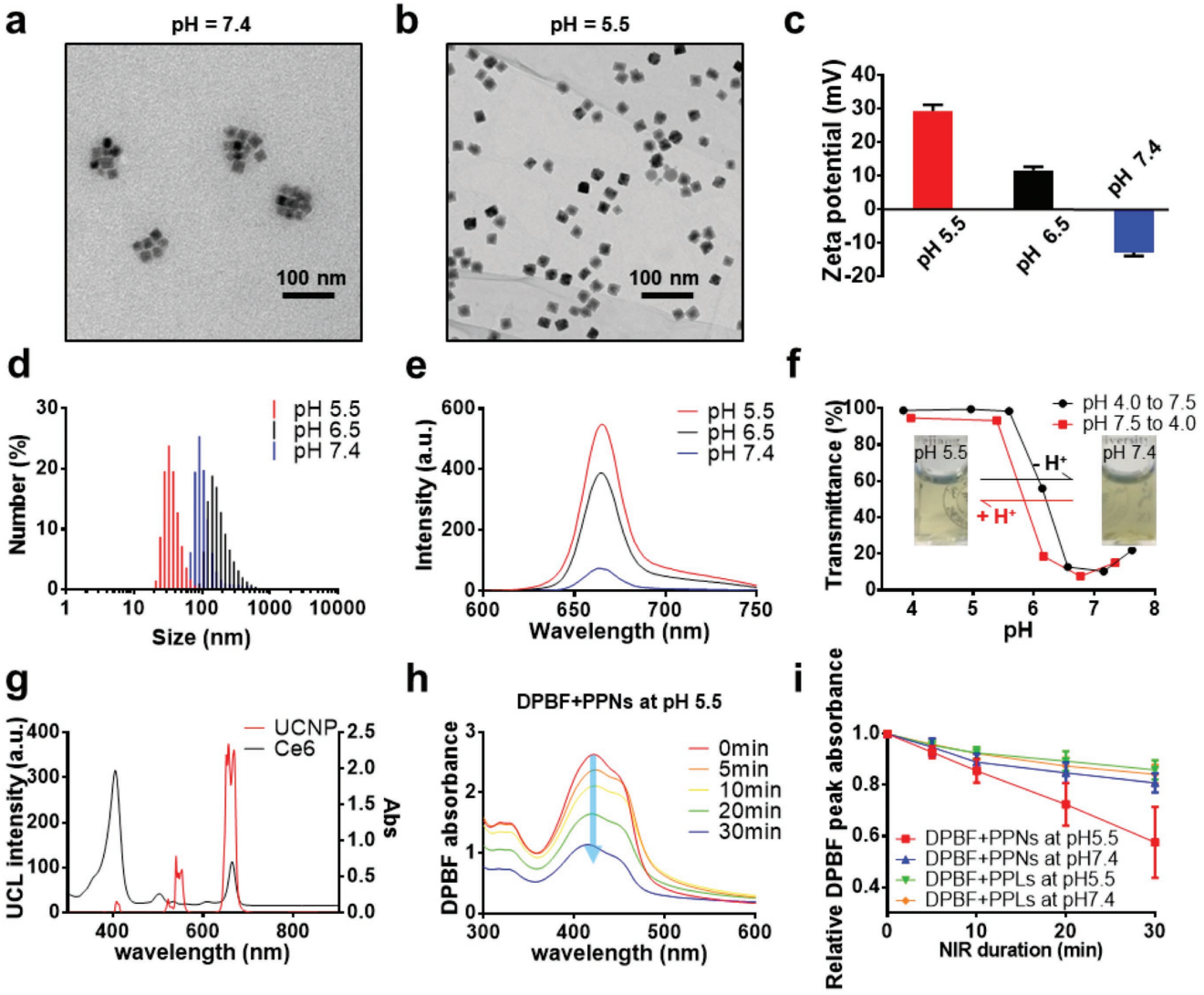

Figure 2. Characterization of PPNs. a) TEM image of PPNs at pH 7.4. b) TEM image of PPNs at pH 5.5. c) Changes in the zeta potential of PPNs at indicated pH values. d) Particle size distribution of PPNs at selected pH values. e) Fluorescence intensity of Ce6 from PPNs at different pH values (Ex = 400 nm, Em = 670 nm). f) pH-dependent changes in transmittance of PPNs. Inset: photographs of PPNs at different pH values. g) UCL spectrum of α-$NaYF_4$:Yb(80%), Er(2%)@CaF_2 core@shell nanoparticles and absorbance spectrum of Ce6. h) Changes in the DPBF absorbance spectra in the presence of PPNs at pH 5.5 under 980 nm laser irradiation over various time durations. i) pH-dependent DPBF absorbance in the presence of PPNs or PPLs under 980 nm laser irradiation at different pH values. Error bars represent standard deviation (n = 3 per group).

FDA-approved surfactant,[15] was added to the mixture containing the PPLs-modified UCNPs to confer the assembled PPNs with colloidal stability in a neutral solution. Finally, excess ligands were removed by centrifugation, and the obtained nanoagents were dispersed in phosphate-buffered saline (PBS). More detailed synthetic routes and characterizations are described in the supporting information (Figures S1–S8, Supporting Information). The pH-insensitive photodynamic nanoagents (PIPNs) were prepared as a control using a similar synthetic process, but utilizing imidazole-free ligands.

As shown in transmission electron microscopy (TEM) images (**Figure 2**a,b; Figure S9, Supporting Information), several UCNPs are assembled to form PPNs at pH 7.4 and disassembled into isolated UCNPs at acidic condition. The PPNs are negatively charged (Figure 2c) with a hydrodynamic diameter of ≈120 nm (Figure 2d) at pH 7.4, where the fluorescence intensity and photoactivity of Ce6 in PPNs is largely quenched due to their close proximity to one another (Figure 2e).[16,17] Once the pH decreases to ≈6.5 in the tumor microenvironment, PPNs quickly reverse their charge to positive because of ionization of the imidazole groups (pK_a ≈ 6.8). This charge reversal not only facilitates the uptake of the positively charged PPNs to tumor cells,[18] but also significantly enhances the electrostatic repulsive force between the UCNPs inside the PPNs. As a result, PPNs begin to swell and partially dissociate (Figure 2d; Figure S9, Supporting Information), and when the pH further decreases to 5.5, the hydrophobic interactions inside the PPNs become weaker than the repulsive force between ionized unimers, leading to the complete dissociation of the PPNs (Figure 2b,d). As pH decreases from 7.4 to 5.5, the average

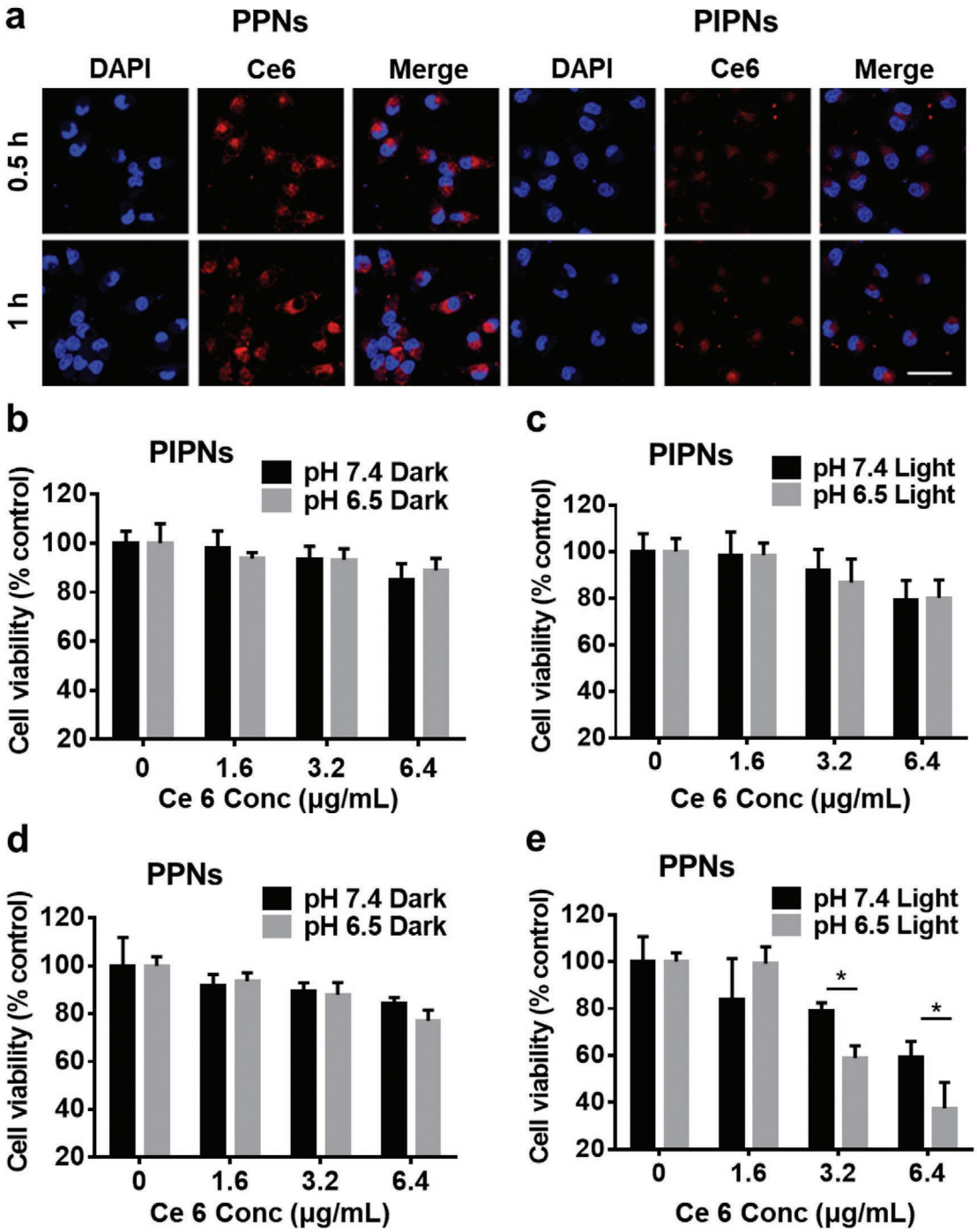

Figure 3. pH-dependent interactions with cells in vitro. a) Confocal laser scanning microscopic studies to demonstrate the cellular uptake of PPNs and PIPNs under mild acid environment (pH 6.5). Cells stained with DAPI are shown in blue, and fluorescence signals from Ce6 in PPNs or PIPNs are shown in red (scale bar = 50 μm). b) CCK-8 assays of A549 cells exposed to PIPNs without 980 nm laser irradiation at either pH 6.5 or 7.4. c) CCK-8 assays of A549 cells exposed to PIPNs with 980 nm laser irradiation at either pH 6.5 or 7.4. d) CCK-8 assays of A549 cells exposed to PPNs without 980 nm laser irradiation at either pH 6.5 or 7.4. e) CCK-8 assays of A549 cells exposed to PPNs with 980 nm laser irradiation at either pH 6.5 or 7.4. (the indicated concentrations represent the concentration of Ce6 in PIPNs or PPNs). The values represent mean ± standard deviation (SD). ($n = 6$ per group). $^*P < 0.05$ as compared to other groups according to multiple t tests.

distance between Ce6 molecules increases, resulting in the recovery of Ce6 fluorescence intensity and photoactivity of PPNs (Figure 2e). The disassembly process is further studied by monitoring spectral changes. As pH value decreases, the absorbance of PPNs is gradually declined (Figure S10, Supporting Information) due to the increased transmittance (Figure 2f), while the UCL from PPNs is increased due to the reduced resonance energy transfer (Figure S10, Supporting

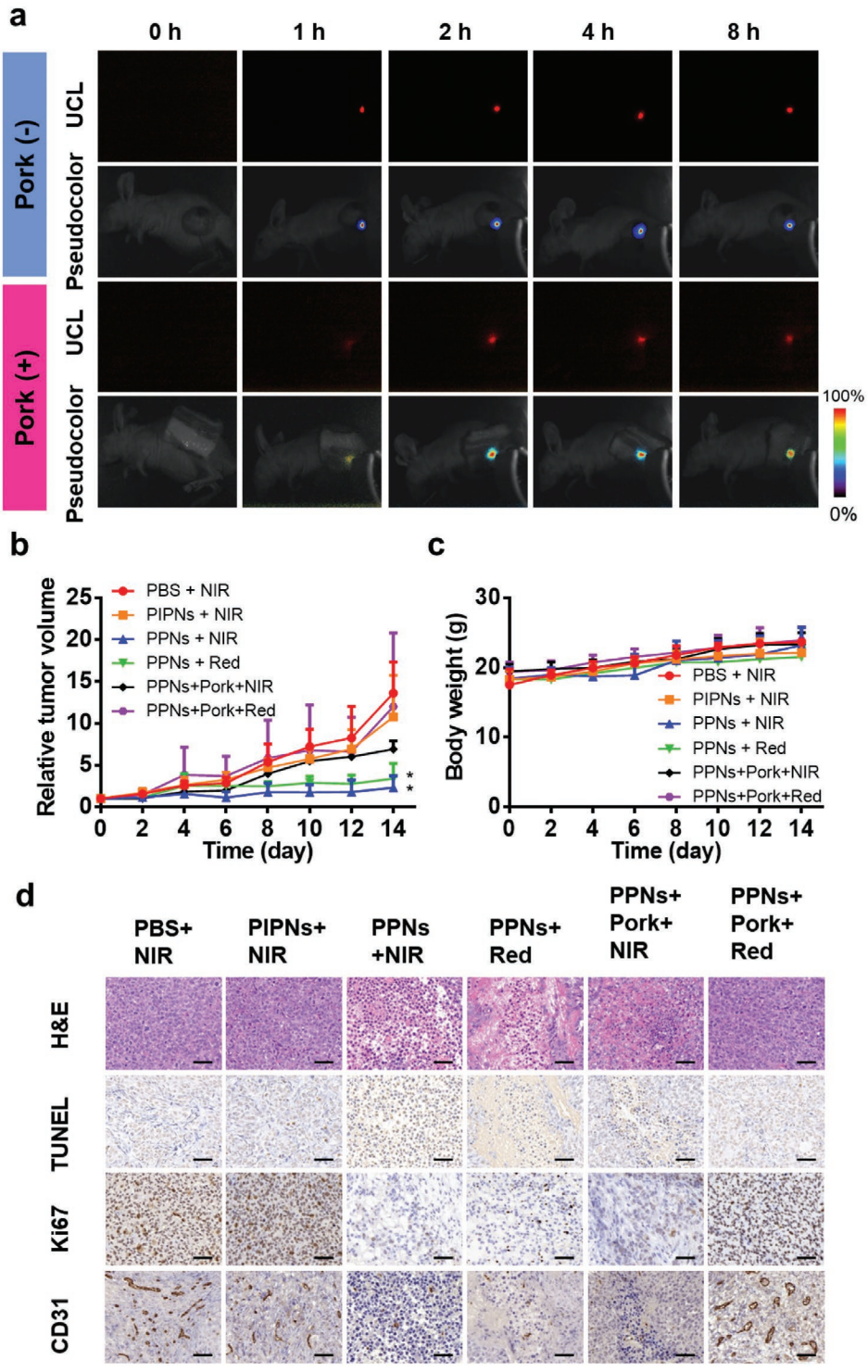

Figure 4. UCL-imaging-guided PDT in vivo. a) In vivo UCL images of mice injected with PPNs, showing corresponding color-mapping-merged images (upper) and those involving tumors covered with pork tissues (lower). b) Relative tumor volume (V_d/V_0) changes in the indicated groups during treatment. $^*P < 0.05$ as compared to PBS groups according to a one-way analysis of variance (ANOVA) test. c) Body weight changes in the indicated groups during treatment. Data represent mean ± standard deviation (SD) ($n = 4$ mice per group). d) Pathological analysis of tumor-inhibitory effects. Representative H&E, TUNEL, Ki67, and CD31 staining of tumor sections collected from different groups at 14 days post-PDT treatment (scale bar = 100 µm).

Information). All these results demonstrate the pH-responsive assembly/disassembly property of PPNs. It is worth mentioning that such assembly/disassembly processes are fully reversible (Figure 2f). By contrast, the size and fluorescence properties of PIPNs are not dependent on pH (Figure S11, Supporting Information).

We then investigated whether the UCL from the UCNPs can excite free Ce6 molecules under acidic conditions. As shown in Figure 2g, red emission from UCNPs matches one of the absorbance peaks of Ce6, indicating that UCNPs can be potentially used as transducers for Ce6 activation. Moreover, we used 1,3-diphenylisobenzofuran (DPBF) to investigate the NIR-triggered singlet-oxygen-generation of PPNs.[19] In aqueous solution (pH 7.4) containing PPNs or PPLs, the DPBF-absorption intensity shows only a slight decrease under NIR irradiation (Figure S12, Supporting Information). In sharp contrast, the DPBF-absorption intensity continuously decreases along with increasing NIR durations (pH 5.5) (Figure 2h,i). This data reflect the pH-activated PDT on/off behavior of the PPNs upon repeatedly switching pH between 5.5 and 7.4 (Figure S10d, Supporting Information).

To validate the feasibility of using PPNs for pH-activated and NIR-triggered PDT, we incubated A549 cells with PPNs or PIPNs. As shown in **Figure 3**a, more intense Ce6 fluorescence signal is observed in the cytoplasm of PPNs-treated A549 cells as compared with that of PIPNs. Moreover, the signal is more intense for the PPNs-treated cells incubated at pH 6.5 rather than pH 7.4 (Figure S13, Supporting Information). These results show that our PPNs are efficient for tumor-cell internalization under mild acidic conditions. Furthermore, we evaluated pH-responsive PDT efficiency in vitro by first verifying that both PPNs and PIPNs exhibit no noticeable cytotoxicity to cells without laser irradiation at either pH 6.5 or 7.4 (Figure 3b,d). Regardless of different pH values, there is no significant difference in cell viability under NIR irradiation for the PIPNs-treated cells (Figure 3c). In sharp contrast, PPNs-incubated cells show significantly elevated death rates at pH 6.5 as compared with the cells at pH 7.4 (Figure 3e). These results clearly demonstrate that both enhanced cell internalization and acidic pH-activated disassembly of PPNs contribute to the enhanced PDT in vitro.

We then assessed the potential of PPNs for in vivo deep tissue PDT by intratumorally injecting PPNs into A549 tumor-bearing nude BALB/c mice. As shown in **Figure 4**a, strong UCL signals were observed at the tumor sites, even at 8 h postinjection, clearly indicating the high uptake efficiency of the PPNs in the tumor. Moreover, the strong UCL signal could still be detected, even when a 7-mm-thick pork tissue was placed over the tumor to simulate a deep tumor, indicating that PPNs could be used for deep-seated tumor imaging. In addition, such a strong UCL signal will greatly facilitate the focus of NIR light only on tumor sites and enhance the accuracy of PDT. We then evaluated the antitumor efficacy of the PPNs for deep-seated tumors by comparing relative tumor size upon light irradiation with that of the control group. As shown in Figure 4b, both the NIR- and red-light-irradiated groups showed similarly high antitumor effects, whereas those treated with either PBS or PIPNs showed no obvious antitumor effects. Compared with PPNs + Pork + Red group, the PPNs + Pork + NIR group exhibited higher antitumor efficacy, with a relative tumor volume of 6.9 versus 11.8 at 14 days postinjection, indicating that NIR is more effective for deep tumor treatment. Additionally, the body weight of mice did not show obvious changes (Figure 4c), indicating the high biocompatibility of the PPNs.

Furthermore, therapeutic efficacy in terms of cancer cell death was evaluated by histological analysis of tumor tissues (Figure 4d). Images of tumor slices stained with hematoxylin and eosin showed significant cancer-cell damage in the groups harboring NIR- or red-light-irradiated PPNs, whereas cells in both the PBS and PIPN groups largely retained their normal morphology.[20] Importantly, we were still able to observe clear cancer cell damage for the group where tumors were covered with 7-mm-thick pork tissues and irradiated with NIR. By contrast, the pork-tissue-covered red-light-irradiation group did not show any obvious cell damage, again indicating that NIR-light excitation is preferable for deep-tumor PDT. Additionally, terminal deoxynucleotidyl transferase dUTP nick end labeling (TUNEL), Ki-67, and CD31 immunolabeling reveal enhanced cancer cell apoptosis and inhibition of proliferation following PPNs + Pork + NIR treatment relative to those observed following PPNs + Pork + Red treatment. All these results clearly show that NIR-triggered pH-sensitive PDT has the highest anticancer efficacy than other treatments.

In conclusion, we developed a pH-activated and NIR-triggered photodynamic nanoagent based on the controlled assembly of photosensitizers grafted pH-responsive polymeric ligands and UCNPs for the targeted PDT of deep-seated tumors. Under a mildly acidic tumor microenvironment, PPNs charge reversal efficiently enhanced their cellular internalization. Subsequently, complete PPNs disassembly at lower endosomal pH levels facilitated the photoactivation of the polymeric PSs. Both in vitro and in vivo results indicate that these PPNs can serve as a potentially new class of PDT agent for use in future cancer theranostics based on their ability to overcome limitations associated with conventional PSs, such as limited tissue-penetration depth, deficiencies in tumor-cell-targeting ability, and inevitable side effects observed in normal tissues.

Supporting Information

Supporting Information is available from the Wiley Online Library or from the author.

Acknowledgements

F.L., Y.D., and J.L. contributed equally to this work. The authors acknowledge financial support by the National Key Research and Development Program of China (2016YFA0203600), the National Natural Science Foundation of China (51503180, 51703195, and 51611540345), "Thousand Talents Program" for Distinguished Young Scholars (588020*G81501/048), Fundamental Research Funds for the Central Universities (520002*172210161), and the Research Center Program for the Institute of Basic Science in Korea (IBS-R006-D1). The animal experimental protocol was performed with the approval of the Institutional Animal Care and Use Committee of Zhejiang University School of Medicine (Protocol No. ZJU20170739) and followed the National Guidelines for Animal Protection.

Conflict of Interest

The authors declare no conflict of interest.

Keywords

nanoassembly, photodynamic therapy, pH-responsive, theranostics, upconversion nanoparticle

Received: May 2, 2018
Revised: June 10, 2018
Published online:

[1] a) D. E. J. G. J. Dolmans, D. Fukumura, R. K. Jain, *Nat. Rev. Cancer* **2003**, *3*, 380; b) J. P. Celli, B. Q. Spring, I. Rizvi, C. L. Evans, K. S. Samkoe, S. Verma, B. W. Pogue, T. Hasan, *Chem. Rev.* **2010**, *110*, 2795.
[2] W. Fan, P. Huang, X. Chen, *Chem. Soc. Rev.* **2016**, *45*, 6488.
[3] a) F. Wang, X. Liu, *Chem. Soc. Rev.* **2009**, *38*, 976; b) M. Haase, H. Schafer, *Angew. Chem., Int. Ed.* **2011**, *50*, 5808; c) G. Chen, H. Qiu, P. N. Prasad, X. Chen, *Chem. Rev.* **2014**, *114*, 5161; d) N. Wang, X. Yu, K. Zhang, C. A. Mirkin, J. Li, *J. Am. Chem. Soc.* **2017**, *139*, 12354; e) D. J. Gargas, E. M. Chan, A. D. Ostrowski, S. Aloni, M. V. Altoe, E. S. Barnard, B. Sanii, J. J. Urban, D. J. Milliron, B. E. Cohen, P. J. Schuck, *Nat. Nanotechnol.* **2014**, *9*, 300.
[4] a) Y. I. Park, K. T. Lee, Y. D. Suh, T. Hyeon, *Chem. Soc. Rev.* **2015**, *44*, 1302; b) S. Wu, G. Han, D. J. Milliron, S. Aloni, V. Altoe, D. V. Talapin, B. E. Cohen, P. J. Schuck, A. P. Alivisatos, *Proc. Natl. Acad. Sci. USA* **2009**, *106*, 10917; c) E. M. Chan, E. S. Levy, B. E. Cohen, *Adv. Mater.* **2015**, *27*, 5753.
[5] a) N. M. Idris, M. K. Gnanasammandhan, J. Zhang, P. C. Ho, R. Mahendran, Y. Zhang, *Nat. Med.* **2012**, *18*, 1580; b) Y. I. Park, H. M. Kim, J. H. Kim, K. C. Moon, B. Yoo, K. T. Lee, N. Lee, Y. Choi, W. Park, D. Ling, K. Na, W. K. Moon, S. H. Choi, H. S. Park, S. Y. Yoon, Y. D. Suh, S. H. Lee, T. Hyeon, *Adv. Mater.* **2012**, *24*, 5755; c) C. Wang, H. Tao, L. Cheng, Z. Liu, *Biomaterials* **2011**, *32*, 6145; d) N. M. Idris, M. K. G. Jayakumar, A. Bansal, Y. Zhang, *Chem. Soc. Rev.* **2015**, *44*, 1449; e) Q. Yuan, Y. Wu, J. Wang, D. Lu, Z. Zhao, T. Liu, X. Zhang, W. Tan, *Angew. Chem., Int. Ed.* **2013**, *52*, 13965.
[6] a) L. Cheng, C. Wang, L. Feng, K. Yang, Z. Liu, *Chem. Rev.* **2014**, *114*, 10869; b) S. S. Lucky, K. C. Soo, Y. Zhang, *Chem. Rev.* **2015**, *115*, 1990.
[7] P. Agostinis, K. Berg, K. A. Cengel, T. H. Foster, A. W. Girotti, S. O. Gollnick, S. M. Hahn, M. R. Hamblin, A. Juzeniene, D. Kessel, M. Korbelik, J. Moan, P. Mroz, D. Nowis, J. Piette, B. C. Wilson, J. Golab, *Ca-Cancer J. Clin.* **2011**, *61*, 250.
[8] a) Z. Zhou, J. Song, L. Nie, X. Chen, *Chem. Soc. Rev.* **2016**, *45*, 6597; b) J. F. Lovell, T. W. B. Liu, J. Chen, G. Zheng, *Chem. Rev.* **2010**, *110*, 2839.
[9] F. Li, J. Lu, X. Kong, T. Hyeon, D. Ling, *Adv. Mater.* **2017**, *29*, 1605897.
[10] a) S. Y. Park, H. J. Baik, Y. T. Oh, K. T. Oh, Y. S. Youn, E. S. Lee, *Angew. Chem., Int. Ed.* **2011**, *50*, 1644; b) S. O. McDonnell, M. J. Hall, L. T. Allen, A. Byrne, W. M. Gallagher, D. F. O'Shea, *J. Am. Chem. Soc.* **2005**, *127*, 16360; c) J. Tian, L. Ding, H.-J. Xu, Z. Shen, H. Ju, L. Jia, L. Bao, J.-S. Yu, *J. Am. Chem. Soc.* **2013**, *135*, 18850; d) D. Ling, W. Park, S. J. Park, Y. Lu, K. S. Kim, M. J. Hackett, B. H. Kim, H. Yim, Y. S. Jeon, K. Na, T. Hyeon, *J. Am. Chem. Soc.* **2014**, *136*, 5647.
[11] H. Chen, J. Tian, W. He, Z. Guo, *J. Am. Chem. Soc.* **2015**, *137*, 1539.
[12] S. Kolemen, M. Işık, G. M. Kim, D. Kim, H. Geng, M. Buyuktemiz, T. Karatas, X.-F. Zhang, Y. Dede, J. Yoon, E. U. Akkaya, *Angew. Chem., Int. Ed.* **2015**, *54*, 5340.
[13] J. Chen, K. Stefflova, M. J. Niedre, B. C. Wilson, B. Chance, J. D. Glickson, G. Zheng, *J. Am. Chem. Soc.* **2004**, *126*, 11450.
[14] A. Punjabi, X. Wu, A. Tokatliapollon, M. Elrifai, H. Lee, Y. Zhang, C. Wang, Z. Liu, E. M. Chan, C. Duan, *ACS Nano* **2014**, *8*, 10621.
[15] A. G. Floyd, *Pharm. Sci. Technol. Today* **1999**, *2*, 134.
[16] H. L. Kejin Zhou, S. Zhang, X. Huang, Y. Wang, G. Huang, B. D. Sumer, J. Gao, *J. Am. Chem. Soc.* **2012**, *134*, 7803.
[17] W. Park, S. J. Park, S. Cho, H. Shin, Y. S. Jung, B. Lee, K. Na, D. H. Kim, *J. Am. Chem. Soc.* **2016**, *138*, 10734.
[18] a) B. Kim, G. Han, B. J. Toley, C. K. Kim, V. M. Rotello, N. S. Forbes, *Nat. Nanotechnol.* **2010**, *5*, 465; b) J. Z. Du, X. J. Du, C. Q. Mao, J. Wang, *J. Am. Chem. Soc.* **2011**, *133*, 17560; c) Y. Y. Yuan, C. Q. Mao, X. J. Du, J. Z. Du, F. Wang, J. Wang, *Adv. Mater.* **2012**, *24*, 5476.
[19] Y. Liu, Y. Liu, W. Bu, C. Cheng, C. Zuo, Q. Xiao, Y. Sun, D. Ni, C. Zhang, J. Liu, J. Shi, *Angew. Chem., Int. Ed.* **2015**, *54*, 8105.
[20] B. Liu, Y. Chen, C. Li, F. He, Z. Hou, S. Huang, H. Zhu, X. Chen, J. Lin, *Adv. Funct. Mater.* **2015**, *25*, 4717.